AD-A087 209 NAVAL RESEARCH LAB WASHINGTON DC F/G 7/4
PROTON RELAXATION IN 1, 3, 5-TRIAMINO-2, 4, 6-TRINITROBENZENE (--ETC(U)
JUN 80 A N GARROWAY, H A RESING DOE-DE-AP-03-79-SF-1018
UNCLASSIFIED NRL-MR-4250 SBIE-AD-E000 477 NL

END
DATE FILMED
8-80
DTIC

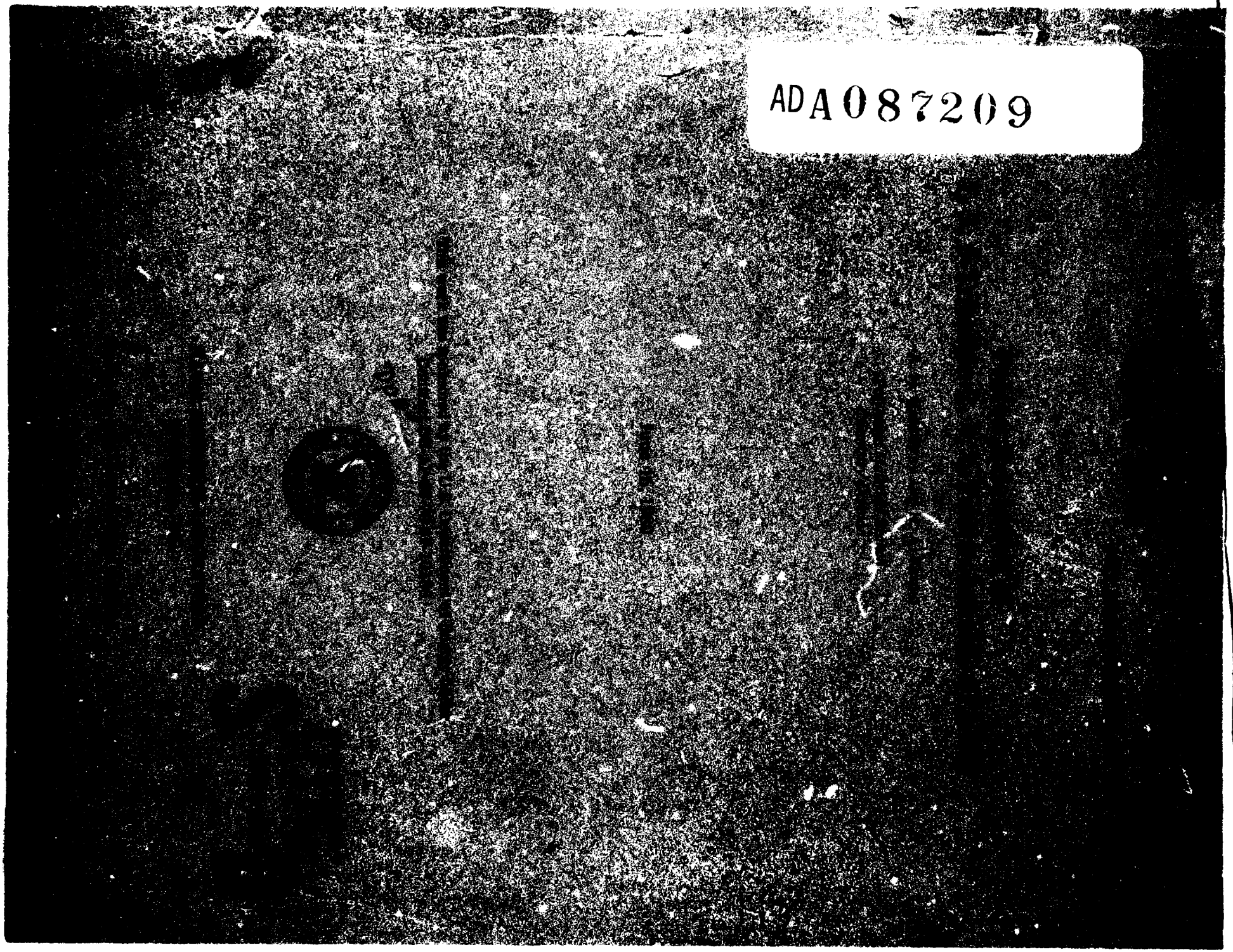

UNCLASSIFIED

SECURITY CLASSIFICATION OF THIS PAGE (When Data Entered)

REPORT DOCUMENTATION PAGE	READ INSTRUCTIONS BEFORE COMPLETING FORM
1. REPORT NUMBER: NRL Memorandum Report 4250 ✓	2. GOVT ACCESSION NO.: AD-A087209 / 3. RECIPIENT'S CATALOG NUMBER:
4. TITLE (and Subtitle): PROTON RELAXATION IN 1, 3, 5-TRIAMINO-2, 4, 6-TRINITROBENZENE (TATB)	5. TYPE OF REPORT & PERIOD COVERED: Final Report 1 April - 31 September 1979
	6. PERFORMING ORG. REPORT NUMBER:
7. AUTHOR(s): A.N. Garroway and H.A. Resing	8. CONTRACT OR GRANT NUMBER(s): DE-AP-03-79-SF-10186
9. PERFORMING ORGANIZATION NAME AND ADDRESS: Naval Research Laboratory ✓ Washington, D.C. 20375	10. PROGRAM ELEMENT, PROJECT, TASK AREA & WORK UNIT NUMBERS: 61-0004-0-0
11. CONTROLLING OFFICE NAME AND ADDRESS: U.S. Department of Energy San Francisco Operations Office 1333 Broadway, Oakland, CA 94612	12. REPORT DATE: 16 June 1980
	13. NUMBER OF PAGES: 24
14. MONITORING AGENCY NAME & ADDRESS (if different from Controlling Office): Lawrence Livermore Laboratory 800 East Avenue Livermore, CA 94550	15. SECURITY CLASS. (of this report): UNCLASSIFIED
	15a. DECLASSIFICATION/DOWNGRADING SCHEDULE:

16. DISTRIBUTION STATEMENT (of this Report)

Approved for public release; distribution unlimited.

17. DISTRIBUTION STATEMENT (of the abstract entered in Block 20, if different from Report)

18. SUPPLEMENTARY NOTES

This work was sponsored by the U.S. Department of Energy under Contract DE-AP-03-79-SF-10186.

19. KEY WORDS (Continue on reverse side if necessary and identify by block number)

NMR
TATB
Triaminotrinitrobenzene
Proton NMR relaxation
Energetic material

20. ABSTRACT (Continue on reverse side if necessary and identify by block number)

Proton nuclear magnetic resonance (NMR) relaxation times have been determined for the compound 1,3,5-triamino-2,4,6-trinitrobenzene (TATB) over the temperature range of approximately -80 to 240 C. The spin-spin (T_2) and Zeeman spin-lattice (T_1) relaxation times are virtually temperature independent, while the dipolar spin-lattice relaxation time (T_{1D}) and rotating frame spin-lattice ($T_{1\rho}$) drop rapidly above about 150 C. The temperature dependence of these relaxation times determines an activation enthalpy for the

DD FORM 1 JAN 73 1473 EDITION OF 1 NOV 65 IS OBSOLETE
S/N 0102-LF-014-6601

UNCLASSIFIED
SECURITY CLASSIFICATION OF THIS PAGE (When Data Entered)

molecular process responsible. The associated jump time can be inferred only on the basis of a specific model for the motion. By a reasonable estimate of the relation between T_{1D} and the jump time τ, we characterize the motion responsible for the high temperature relaxation by the jump time.

$$\tau \simeq 2 \times 10^{-16} \exp (120\,000/RT)$$

where τ is in seconds and R in units of J mol^{-1} deg^{-1}.

The motion cannot be unambiguously identified with those results: rotations or 180° flips of the amino protons are possible as well as rotation about the TATB three-fold axis. By comparison with other molecules, we can, however, rule out translational diffusion as the motion contributing to this relaxation above 150°C.

The proton NMR spectrum shows the characteristic Pake doublet due to the nearly isolated proton pairs of the amino groups. The observed dipolar splitting predicts an "average" amino proton separation of 0.185 ± 0.001 nm, in contrast to previous x-ray results of 0.1553, 0.1577 and 0.1726 ± 0.02 nm for the three distinct pairs in TATB.

CONTENTS

PROTON RELAXATION IN 1,3,5-TRIAMINO-2,4,6-TRINITROBENZENE (TATB)

I. INTRODUCTION

The compound 1,3,5 triamino-2,4,6-trinitrobenzene (TATB) is simple yet intractable; it is virtually insoluble and sublimes with decomposition at elevated temperature. It is, however, extremely attractive in its role as an insensitive high explosive. The origin of this insensitivity is not presently known.

Compressed powders of pure TATB and also plastic bonded TATB materials are found to expand irreversibly when the temperature is cycled; it is suggested (1) that this hysteresis stems from stresses induced by the anisotropic volume expansion of TATB. The mechanism for the large c-axis thermal expansion coefficient, over eight times that of graphite, is not understood.

As a step towards identifying the character of the molecular motions which may relate to mechanical insensitivity and thermal expansion, we have performed a series of proton relaxation studies in (solid) TATB over the temperature range of approximately -80 to 240°C. In brief, we find that there is very little (detectable) molecular motion below about 150°C. From about 150 to 200°C we observe a motion with an activation enthalpy of 120 kJ/mol and associated frequency prefactor of 0.5×10^{16} Hz. At 205°C, this corresponds to a jump time of around 5 ms, while at room temperature five days elapses between those jumps. We find this activation enthalpy is too small for translational diffusion; the motion may involve large angle libration or rotation of the amino group or in-plane rotation of the entire molecule, though other mechanisms are not ruled out by these data. In particular, we observe no evidence for nonsubtle changes either in the crystal structure or in the nature of the molecular motions in the temperature range around 30°C. Relaxation data at elevated temperatures up to the decomposition point (350°C) might help to distinguish further among the possible models for motion in TATB.

II. EXPERIMENTAL

TATB powder (micronized, chlorine-free) was obtained from J. R. Kolb of the Lawrence Livermore Laboratory. In the as-received material, a narrow proton NMR line near the center of the Pake doublet is

Manuscript submitted April 23, 1980

ascribed to liquid water (see Section III). This water was removed by heating the samples to 200°C for 0.5 to 2 hours under vacuum; a 0.1% weight loss occurred.

For the T_2, T_1 and T_{1D} relaxation data, the pumped powder was then compressed into pellets (0.55 cm dia x 1.2 cm) under about 14MPa (2000 psi) pressure. Samples fit into glass tubes; a copper-constantan thermocouple junction was suspended about 1 cm above the pellet and the sample tube was nominally sealed off by a stopper.

For technical reasons, a separate probe was used for the few $T_{1\rho}$ measurements reported here. In this case a separate pumped specimen was pressed into a 1.25 cm dia x 3 cm cylinder. Thermocouples were placed in access ports of the heavy copper probe body; subsequent bench tests showed these reflected the temperature within the sample coil to better than 3°C. Few $T_{1\rho}$ data are presented; the sample degraded at about 300°C, and damaged the probe.

A Bruker SXP NMR spectrometer was used. For the T_2, T_1 and T_{1D} measurements, the proton Larmor frequency was 60 MHz and the rf field strength was 150-200 kHz. (Field strengths are reported in frequency units by the relation $f=\gamma_H B/2\pi$, where B is the field and γ_H the proton magnetogyric ratio.) A special probe was required for the $T_{1\rho}$ measurements; this operated at 25 MHz and a spin-lock rf pulse amplitude of 50 kHz was selected.

The T_2 data were determined by the zero crossing of the free induction decay (fid). To minimize receiver recovery time, the fid was observed immediately following a spin-locking sequence consisting of a $\pi/2$ pulse and a 100μs phase-shifted spin-lock pulse. The phase of the initial $\pi/2$ pulse was alternately changed by 180° while the signal was synchronously added and subtracted to computer memory; this was done to discriminate against instrumental transients and in favor of the nuclear signal. The start of the fid was considered to occur at the very end of the spin-lock pulse.

The solid echo pulse sequence, $\pi/2(0^\circ)-\tau-\pi/2(90^\circ)-\tau$-echo, was not satisfactory for T_2 determination. (In this notation, the figures in parenthesis give the relative rf phase.) Though the echo refocussing at the time 2τ is perfect for an isolated spin pair (2,3), the amino proton pairs in TATB are not completely isolated. Many of the contributions to the fid time evolution which arise from outside the spin pair will lead to a systematic error in the fid zero crossing (3).

The dipolar spin-lattice relaxation time T_{1D} was determined by the two pulse method of Jeener and Broekaert (4), $\pi/2(0^\circ)-\tau-\pi/4(90^\circ)-t-\pi/4(90^\circ)$. The separation τ between the first two preparation pulses is to coincide with the steepest part of the fid; τ was set to 12 μs, as measured between the rising edges of the pulses. As above, the phase of the first pulse was alternated from 0° to 180° to reduce transients.

In TATB, the proton Zeeman spin-lattice (longitudinal) relaxation time T_1 is quite long, of the order of 30 sec. In the T_2, T_{1D} and $T_{1\rho}$ experiments, the magnetization was not allowed to return to its thermal equilibrium value. Instead, to avoid any ambiguity about what magnetization was inspected by the sequence, each sequence began by destroying all magnetization along the B_o (z) axis by a comb of 12 $\pi/2$ pulses spaced 80 μsec apart. Then a 10 sec delay was allowed for the magnetization to recover.

The T_1 determination proceeded also by destroying magnetization by the 12 pulse comb and then monitoring the magnetization recovery of a two-pulse solid echo.

For $T_{1\rho}$, the decay of the fid was monitored for varying spin-lock pulse lengths, at constant rf field of 50 kHz. The rf field dependence was not studied here.

III. RESULTS AND DISCUSSION

A. Spin-spin Relaxation (T_2)

The proton NMR spectrum of TATB is shown in Fig. 1; the narrow water peak in the as-received material (a) has essentially disappeared after heating at 200°C under vacuum (b) with a concomitant weight loss of 0.1%. In Fig. 1 the linewidth of the narrow resonance is artifically broad, due to truncation of the free induction decay (fid). Other spectra (not shown) obtained with a longer acquisition time give a more realistic value for the linewidth of 700±50 Hz. This is substantially greater than magnet inhomogenity (40Hz) or bulk susceptibility effects. We infer that the narrow resonance arises from water which is partially constrained by the TATB powder. The water peak at δ=4.1±0.8 ppm (relative to TMS) is essentially unshifted from neat water at δ=4.7 ppm.

The spectrum of Fig. 1b represents the classical and characteristic Pake doublet (5), here arising from the dipolar coupling of the amino proton pair; the spectrum is broadened slightly by mechanisms discussed below. The center of the spectrum is shifted approximately 34±8 ppm downfield from TMS. This shift, also observed in TATB by Fukushima (6), reflects the substantial hydrogen bonding in the crystal.

We look for any change with temperature in the dipolar coupling; such a change indicates the presence of a molecular motion modulating the coupling at a frequency greater than or equal to the coupling frequency (about 30kHz for the dominant splitting in the Pake doublet). Now, Fig. 1 is not a perfectly faithful rendition of the TATB spectrum; all such spectra are distorted by imperfections arising from the overloading of the NMR receiver following the end of the rf transmitter pulse. Here that overload time is 6.5 μs. As an alternative to comparing details of distorted spectra, it is more convenient instead to characterize the entire spectrum by the first zero crossing of the fid and also by the average spectral broadening produced by dipolar coupling outside the amino group. For a single Pake doublet (e.g. for a powder of proton pairs, each with identical

intra-pair distance), the time dependence of the normalized free induction decay is (7)

$$G(t) = \exp\left[-1/2\,\beta^2 t^2\right] f(\alpha t), \qquad [1]$$

where

$$f(\alpha t) = \alpha(8\pi)^{1/2}\left\{\frac{\cos\alpha t}{(\alpha t)^{1/2}}\,C\,(z^{1/2}) + \frac{\sin\alpha t}{(\alpha t)^{1/2}}\,S(z^{1/2})\right\}. \qquad [2]$$

Here $(4/5)\,\alpha^2$ is the second moment of the intra-pair coupling and

$$\alpha = 3\gamma^2\hbar/(4r^3), \qquad [3]$$

where r is the pair separation. The second moment contribution of all the other spins (the extra-pair contribution) is β^2 and by assumption its contribution to the fid is Gaussian as in Eq. [1]. The argument of the Fresnel sine and cosine integrals S and C is $z \equiv 6\alpha t/\pi$.

The advantage of the zero crossing measurement ($G(t_o)=0$) is easily seen from Eq. [1]: the zeros of G(t) are determined completely by the intra-pair coupling α. Further, the first zero crossing occurs at $t_o = 2.160/\alpha$; the experimental value for TATB is $t_o \simeq 25\mu s$ and the zero crossing event is well-removed from the receiver recovery period; thus t_o is less subject to error than the splitting in the Pake spectrum. Once α is experimentally determined, the extra-pair contributions (β^2) can then be determined by dividing G(t) by $f(\alpha t)$.

For a pumped, compressed powder of TATB we have determined the first zero crossing with its associated intra- pair second moment as a function of temperature. The second moment results are shown in Fig. 2 and Table I while zero crossing data is also collected in Fig. 5. The intra-pair second moment ranges from 8 to 10 G^2 while the extra- pair contribution is about $3G^2$. The second moments are essentially temperature independent over the range -80 to 230°C, indicating that in this temperature range there is no motion which modulates the dipolar couplings at a rate greater or equal to the dipolar coupling frequency of about 30 kHz. (For example, if the TATB molecule were rotating rapidly about its three-fold axis, the intra-pair second moment would drop by a factor of four, as would any other intramolecular contributions). While there is a substantial thermal expansion along the c-axis in TATB, the proton pairs are essentially in the ab plane and their separation is less sensitive to thermal expansion. Using the position vectors of Cady and Larson (8) and the temperature dependence of the unit cell parameters of Kolb and Risso (1), we have calculated that there is less than a 2% change expected in the intra-pair second moment over the temperature range -26 to 230°C. Although no x-ray data are available for 104 to 230°C, in this range we used the average expansion

coefficients over -54 to 104°C together with the values of the unit cell angles for 104°C.

From the experimental value of the intra-pair second moment, we can infer the pair separation via Eq. [3]. At 26°C the zero crossing time is 24.2±0.5μs corresponding to an intra-pair second moment of 8.9 ± 0.4G^2; the experimental value for the extra-pair moment is 3.1±0.5 G^2, calculated by the route just described. The pair separation is then 0.185 ± 0.001 nm. This value, which presumes a single value for all the pair separations, may be compared to the x-ray results of Cady and Larson (8). There the proton separations in the three amino groups are 0.1553, 0.1577 and 0.1726 ± 0.02 nm, where we have calculated the separations from the atomic position vectors given by the spherical refinement of Ref. 8. The proton distances are rather poorly identified by the x-ray data and from the quoted errors in the position vectors (8) we infer that the associated error in the pair separation is approximately ± 0.02 nm, for each pair, as indicated. Intra-pair second moments based on the x-ray determined separations are shown in Table I. The NMR estimate of 0.185 ± 0.001 nm is consistent with one of the x-ray values and slightly outside the range of uncertainty for the two other pairs.

As the uncertainty in the x-ray determined proton separations is so large, it is unclear that there are actually three widely different pair separations and so no attempt was made here to scrutinize the NMR spectra for the presence of three distinct pairs. If the pair separation were not unique, then the zero crossing time would represent an intermediate average over the three pair contributions to the fid. As all of the x-ray distances fall below the NMR determination, we infer that some if not all the x-ray proton pair separations are too short.

We have calculated the extra-pair proton-proton second moment from the x-ray data: by definition this is the second moment contribution to each of the six distinct TATB amino protons made by all other protons in the crystal but excludes the proton within each respective pair. The average over the six protons is just the extra-pair contribution to the total proton second moment. The contributions of near neighbors out to 1.01 nm were considered and we estimate this truncation underrepresents the actual second moment by no more than 3%. The extra-pair second moments are presented in Table I for protons numbered 1-6 in the notation of Ref. 8. These moments are more reliable than the intra-pair moments, as they involve the well-determined unit cell dimensions in addition to less-determined intramolecular proton distances. The average extra-pair interaction is 1.50 G^2 which is substantially less than the 3G^2 measured experimentally (Fig. 2).

However, the dipolar field of the amino nitrogen may also contribute to the proton second moment. The magnitude of the ^{14}N-^{1}H coupling is difficult to assign for a number of reasons. As the ^{14}N nucleus has a quadrupole moment and sees a very unsymmetrical electronic environment in TATB, the quadrupolar splitting is probably of the order of 1-3MHz, which is not too different than the ^{14}N Larmor frequency of 4.3 MHz at this magnetic field. Hence the nitrogen spin is not quantized along the

B_o axis and any calculated rigid lattice second moment which assumes B_o quantization will be too low (9). Secondly, molecular motion will lead to rapid ^{14}N relaxation and this relaxation will motionally average and so diminish the ^{14}N-^{1}H interaction. Finally, the N-H x-ray distances are not very reliable. With these caveats, we therefore present in Table I naive estimates of the ^{14}N contribution to the proton rigid lattice second moment; the indicated errors reflect the quoted uncertainty in the x-ray distances only. The average ^{14}N-^{1}H contribution is $4.3\pm1G^2$, greater than the difference between the observed extra-pair moment ($3.1G^2$) and the calculated $1.50G^2$ extra-pair proton-proton contribution. This result may also suggest the x-ray N-H distances are somewhat short.

More information can be extracted. If the three proton pair separations were markedly different as indicated by the x-ray results, then the resulting proton spectrum would correspond to three Pake doublets of different widths. The zero crossing technique measures some intermediate pair separation; moreover, when the extra-pair spectral broadening is determined by dividing out the intra-pair fid of Eq. [2], then any deviations from a unique Pake splitting will appear as an apparent extraneous broadening. We can roughly estimate the second moment of apparent broadening by the standard deviation of the three intra-pair moments inferred from the x-ray distances. The standard deviation is, from Table I, $3G^2$, a value which is too large to account for the difference between the observed extra pair moment ($3.1G^2$) and the calculated proton-proton extra-pair moment ($1.50G^2$).

Thus these NMR second moment results require somewhat larger and more nearly equal proton pair separations than those determined by x-ray. Unfortunately we cannot tell with these data whether the difference between the observed extra-pair second moment and the calculated proton-proton extra-pair moment arises primarily from different Pake splittings or from the ^{14}N-^{1}H contribution to the second moment.

The reconciliation of the x-ray and NMR derived proton separations is not so central to this report. More importantly, as we have already shown, the temperature independence of both the extra-pair and intra-pair second moments rules out from -60 to 230°C any molecular motion which might modulate the dipolar couplings at a rate greater or equal to these dipolar field frequencies. Slower motion proceeds, however, as shown in Section III. C.

B. Zeeman Spin-lattice Relaxation (T_1)

The Zeeman spin-lattice (longitudinal) relaxation time is determined by molecular motions at the Larmor frequency, in this case 60 MHz. For TATB, proton T_1 measurements were performed over -80 to 210°C. In addition, a separate TATB sample was pumped, pressed and then γ-irradiated with a 3 MRad dosage; T_1 was determined for this sample at high and low temperature.

At 113°C the T_1 magnetization data are shown as a semilogarithmic plot in Fig. 3 and as magnetization versus $t^{1/2}$ in Fig. 4. Here the magnetization is measured by sampling the height of the initial portion of the free induction decay: this is proportional to the integrated magnetization across the entire proton spectrum. The decay is clearly nonexponential. For nuclear relaxation induced by rapidly fluctuating electron-nuclear dipolar field of uniformly distributed paramagnetic centers, one naively expects the magnetization to recover as $(t/T_1)^{1/2}$ for short times (10). Of course, other mechanisms and in particular a nonuniform distribution of paramagnetic centers can lead to non-exponential recovery; also, over a sufficiently limited range of magnetization recovery, almost any recovery law can be fit (11). Nevertheless, in Fig. 4 the relation $M \propto (t/T_1)^{1/2}$, with T_1=35 s , better represents the data than does an exponential recovery.

As a test to see if there were a distribution of relaxation times across the TATB spectrum, we examined further these 113°C data as well as the γ-irradiated sample at 211°C. The fids were Fourier transformed and magnetization plotted versus the square root of time for the center of the spectrum, one peak, and one shoulder; in the Pake doublet the shoulder is twice as far off resonance as the peak. The center of the pattern corresponds to proton pairs aligned at 54.7° relative to the static field B_o. The shoulder corresponds to orientations parallel to the field, while the peak is a mixture of 90° and 35.3° orientations. The decays were reasonably fit by a $(t)^{1/2}$ dependence even out to the point that the fractional magnetization had recovered by about one half. The T_1 values corresponding to the one half point (Table II) show a maximum of a 20% variation across the line: for both specimens, the fastest relaxing part of the line corresponds to proton pairs parallel to the field B_o. The longitudinal relaxation time of the irradiated sample has been reduced by over a factor of two from the unirradiated one. It is more convenient to characterize the longitudinal relaxation data at each temperature by a single parameter rather than record the slight T_1 dependence across the spectrum and so we report the T_1 data in Figure 5 as the time for the fid magnetization to recover to one half of its original value.

The T_1 data are essentially temperature independent, though there is perhaps a slight trend towards longer relaxation times at higher temperatures. These long relaxation times, the recovery of the magnetization with nearly a one half power of time and the decrease in T_1 on γ-irradiation all indicate that paramagnetic centers rapidly relax nearby protons nuclear spins; by mutual spin flips the proton magnetization diffuses away from these centers to build up macroscopic magnetization. The slight T_1 temperature dependence may represent less efficient paramagnetic relaxation at higher temperature or a slight reduction in the spin diffusion rate which is proportional to T_2^{-1}.

The virtually temperature independent T_1 values show that there is no substantial molecular motion at high frequencies (60 MHz). We turn now to an experiment sensitive to slower motions.

C. Dipolar Spin-lattice Relaxation (T_{1D})

The rate at which a state of dipolar order relaxes back to the lattice temperature can provide measure of slow and ultra slow molecular motions (12). The decay of dipolar magnetization in TATB is generally nonexponential and we characterize it by the time to decay to the one half value; however, above about 150°C, the decay becomes more and more exponential and for those temperatures we quote also the 1/e time. As shown in Fig. 5, T_{1D} slowly diminishes by about a factor of four from -83 to 115°C and then drops rapidly above 150°C. The shortest T_{1D} (1/e) we observed is 3.7 ms at 205°C.

Dipolar order is relaxed by any motion which alters the instantaneous local dipolar field seen by a nuclear spin. For vacancy diffusion, the general relation is (12)

$$T_{1D} = \frac{\tau_d}{2(1-p_d)} \qquad [4]$$

where τ_d is the molecular jump time and $(1-p_d)$ measures, roughly speaking, the fractional change in the square of the local field due to that diffusional jump. For example, $p_d = 0.266$ for vacancy diffusion to nearest neighbor sites in a powder of body-centered cubic crystallites (12).

For rotation of a spin pair, the relaxation due only to the modulation of the pair interaction is

$$T_{1D} = \frac{\tau_r}{(1-p_r)} \qquad [5]$$

For three-fold reorientation perpendicular to the internuclear spin vector, the value $p_r = -5/22$ holds (12). This analysis would apply for TATP reorientation about the three-fold axis.

Pair exchange (two-fold reorientation) will also modulate the local field arising from nuclei outside the pair, although the efficiency of this relaxation process is reduced. We estimate the efficiency $(1-p_r')$ of this process to be equal to the ratio of the proton-proton extra pair contribution to the second moment ($1.5G^2$ theoretical value) divided by the total proton second moment ($9\ G^2$ experimental intra pair moment plus the $1.5\ G^2$). Hence $1-p_r' \simeq 1/7$ for the-extra pair contribution to dipolar spin-lattice relaxation.

Thus the difference between very efficient three-fold axis reorientation of TATB ($1-p_r = 27/22$) and inefficient 180° amino proton

flips ($1-p_r' = 1/7$) is less than an order of magnitude. So, independently of the details of the motion, we may set $1-p \simeq 1$ in order to use T_{1D} as a direct measure of the molecular correlation time τ of some unspecified molecular process:

$$T_{1D} \simeq \tau = \tau_o \exp H/kT \qquad [6]$$

From a fit of the T_{1D} (1/e values) at the four highest temperatures on Fig. 5, we find: $\tau_o = 2\times10^{-16}$s and H = 120 kJ/mol. The significance of this activation energy is discussed in Section E.

D. Rotating Frame Spin-lattice Relaxation ($T_{1\rho}$)

In Fig. 5 we also show the limited data set for the TATB proton $T_{1\rho}$ for an rf field strength of 50 kHz. As mentioned earlier, the compressed TATB specimen degraded at about 300°C (corresponding $T_{1\rho}$ data are not shown) and damaged the probe, so precluding further experiments.

The decay of rotating frame proton magnetization is found to be nonexponential in TATB and the $T_{1\rho}$ value is quoted as the time for the magnetization to decay to one half of its initial value. The $T_{1\rho}$ values roughly parallel the behavior of T_{1D} and there is a similar drop at high temperature. In Fig. 5 the T_{1D} temperature dependence has been drawn (dashed curve) through the few $T_{1\rho}$ data; the reasonable fit shows that the $T_{1\rho}$ relaxation process is also consistent with the activation enthalpy of 120 kJ/mol.

The magnitude of the $T_{1\rho}$ values is not fully understood. Experimentally, $T_{1\rho}/T_{1D} \simeq 20$ at high temperature ($T \geq 170$°C, $1000/T \leq 2.25$) while for the two $T_{1\rho}$ data at lower temperature, $T_{1\rho}/T_{1D} = 2.5$-3. For illustration only, we consider isotropic reorientation, which is the most efficient dipolar relaxation process.

In a powder of homonuclear spins irradiated on resonance (13),

$$T_{1\rho}^{-1} = M_2 \frac{\tau_c}{1+4\omega_1^2\tau_c^2} \qquad [7]$$

Here M_2 is the second moment modulated by the motion, τ_c the correlation time and ω_1 is the rf field strength in rad/sec. For slow motion, $\omega_1\tau_c >> 1$ and with $T_{1D} \simeq \tau_c$, then

$$T_{1\rho}/T_{1D} \simeq 4\omega_1^2/M_2 \qquad [8]$$

For a total proton second moment of about 12 G^2 (experimental values of 9 G^2 intra-pair and 3.1G^2 extra-pair), Eq. [8] predicts $T_{1\rho}/T_{1D} = 45$, a factor of two greater than that observed. Isotropic reorientation is unlikely to occur in TATB. The more restricted motions are less efficient at producing $T_{1\rho}$ relaxation and also generally less efficient at producing T_{1D} relaxation. A more careful calculation considering the detailed dynamics of possible relaxation mechanisms would be required to extract more information from the experimentally determined ratio $T_{1\rho}/T_{1D}$. TATB is not a simple spin system, involving as it does strongly coupled, possibly inequivalent proton pairs further coupled to the quadrupolar ^{14}N nuclei as well as to the rest of the lattice. For now we note only that at high temperature the observed ratio is broadly consistent with the determination of $T_{1\rho}$ and T_{1D} by a single relaxation time, described by Eq. [6].

At lower temperatures below, say, 150°C, $T_{1\rho}$ is only a few times larger than T_{1D}. Unfortunately from those data we cannot yet determine the $T_{1\rho}$ or T_{1D} relaxation mechanism in this region.

E. Molecular Motion in TATB

From the measurements of T_{1D} at high temperature, where molecular motion dominates the relaxation, we have estimated the jump time for the motional process to be

$$\tau = 2\times10^{-16} \exp\ (120\ 000/RT) \qquad [9]$$

where R is in units of J mol^{-1} deg^{-1} and τ is in seconds. The TATB molecule has various possibilities for molecular motion: translational diffusion, molecular rotation about the three-fold symmetry axis, or even rotation of nitro as well as amino groups. For diffusion, the activation enthalpy for planar molecules is generally somewhat greater than twice the latent heat of sublimation, as exemplified by the entries in Table III for benzene and naphthalene (14). A reliable value for the latent heat of sublimation, ΔH_{sub}, of TATB does not exist in the literature (15). Thus to estimate the activation enthalpy for translational diffusion in TATB ΔH_{sub} itself must be estimated, as is done below in three ways. First, TATB is to a good approximation the same size as coronene, for which experimental and theoretical estimates of ΔH_{sub} exist (Table III), about 140 kJ/mol. (16). Second, from mass spectroscopic measurements, it has been found (15) that TATB begins to show an appreciable vapor pressure (about 10^{-3} torr) at 200°C; use of this datum with the approximate equation (17)

$$\log_{10} p(\text{torr}) = 13 - \Delta H_{sub}/(2.303RT) \quad [10]$$

yields a value of 145 kJ/mol for ΔH_{sub}. Finally, a table (18) of functional group increments for ΔH_{sub} is used to estimate ΔH_{sub} of 180 kJ/mol. Thus the activation enthalpy for diffusion, expected to be about twice ΔH_{sub}, should be about 300 kJ/mol. Since this is much larger than the activation enthalpy of 120 kJ/mol found in this study, the translational diffusion process is eliminated as the source of the high temperature T_{1D} relaxation effect.

In Table III, activation enthalpies for molecular rotation, ΔH_{rot}, are also gathered. Coronene, a molecule with a six-fold axis of symmetry, requires only 25 kJ/mol for rotation (16), while naphthalene, with only a two-fold axis, requires 105 kJ/mol. (16). For neither of these do hydrogen bonding or molecular electric dipole moments play any role in the potential energy function. TATB, with a three-fold axis, and roughly the same moment of inertia as coronene, should resemble coronene, except for the possible contributions of polar groups and hydrogen bonding. Thus 25 kJ/mol is a reasonable lower bound to the enthalpy of activation for rotation in TATB. But a rotation of the amino group by 180° is also a possible contributor to relaxation, though much less effective.

A strategy to discriminate between the two rotational possibilities is a study of relaxation in the rotating reference frame as a function of rf field strength, which we have begun but not yet completed. Further studies at higher temperature may be useful, although limited. Though TATB does not melt until about 440°C (19), the degradation at 350°C (20), as well as the degradation we observed at around 300°C in the compressed sample, provide a very inconvenient ceiling on the accessible temperatures. By extrapolation of our data, we should expect at 300°C that substantial line narrowing will occur as the molecular jump time becomes comparable to the T_2 (zero crossing) time. Further temperature dependent rotating frame relaxation time results would be helpful in assessing the details of the motion, although we estimate that the $T_{1\rho}$ minimum would not occur until about 365°C for the rf field strength of 50 kHz. (The observation of the T_1 minimum is strictly precluded, as it probably occurs at around 575°C.) At lower temperature, nuclear spin echo as well as esr studies could more fully identify the role of ^{14}N relaxation and paramagnetic impurity relaxation.

IV. CONCLUSIONS

Below about 150°C there is no molecular motion in TATB which is detectable by these NMR experiments. The determination of the dipolar spin-lattice relaxation times (T_{1D}), and rotating frame relaxation

times ($T_{1\rho}$), which are extremely sensitive to slow motions, has pointed to a motion with an activation enthalpy of 120 kJ/mol. The correlation time τ for this motion can be extracted from the T_{1D} data only on the assumption of a particular motional model; nonetheless, it is a fair estimate to set $\tau \simeq T_{1D}$ and from this we inferred a prefactor in the Arrhenius relation of 2×10^{-16} s. At room temperature this motion, responsible for the T_{1D} relaxation at high temperature, corresponds to jumps occurring approximately every five days.

The motion responsible for the high temperature (above 150°C) T_{1D} and $T_{1\rho}$ relaxation cannot be unambiguously determined; 180° flips of amino protons and three-fold axis reorientation are possibilities. On comparison with other characterized organic molecules, the activation energy we observe is smaller, by more than a factor of two, than that expected for translational diffusion and so the relaxation data we present is inconsistent with translational diffusion at these temperatures.

The T_2 values and Pake doublet lineshape are characteristic of strongly coupled dipolar pairs which are only weakly linked to the other nuclei in the crystal. As an indication of hydrogen bonding, the proton spectrum is shifted downfield to $\delta = 34 \pm 8$ ppm. On the assumption that the three amino proton pair separations are identical, we infer from the T_2 data a proton separation of 0.185 ± 0.001 nm, a value outside the x-ray results of 0.1553, 0.1577 and 0.1726 ± 0.02 nm; we feel these latter separations are systematically in error.

The broadening of the Pake pattern can be described by a Gaussian with a 3 G^2 second moment. Of this, 1.5 G^2 arises from proton-proton coupling from outside the amino pair. Nitrogen-proton dipolar coupling may account for 4.3 G^2 and a distribution of amino proton pair separations, as given by the x-ray results, could also account for 3 G^2. The experimentally observed broadening indicates that the amino proton pair separations are not so disparate. Both the intra and extra-pair proton second moments are temperature independent over -80 to 230°C.

The Zeeman spin-lattice relaxation times T_1 are also essentially temperature independent in the range accessible and are most likely determined by the relaxation of paramagnetic centers within the crystal.

ACKNOWLEDGEMENTS

Thanks go to our colleagues, W. B. Moniz, A. D. Britt and especially to G. C. Chingas for discussions about the role of free radicals in TATB. Professor Britt also made available unpublished mass spectroscopy data, upon which we have based our estimate for the heat of sublimation of TATB. F. L. Carter kindly aided in analysis of the published x-ray study.

REFERENCES

1. J. R. Kolb and H. F. Rizzo, Propellants and Explosives 4, 10 (1979).

2. J. G. Powles and P. Mansfield, Phys. Lett. 2, 58 (1962).

3. P. Mansfield, Prog. in Nuclear Magnetic Resonance Spectroscopy 8 (J. W. Emsley, J. Feeney and L. H. Sutcliffe, eds.) (Pergamon, Oxford) p. 41 1971.

4. J. Jeener and P. Broekaert, Phys. Rev. 157, 232 (1967).

5. G. E. Pake, J. Chem. Phys. 16, 327 (1948).

6. E. Fukushima (private communication).

7. D. C. Look, I. J. Lowe and J. A. Northby, J. Chem. Phys. 44, 3441 (1966).

8. H. H. Cady and A.C. Larson, Acta. Cryst. 18, 485 (1965).

9. D. L. VanderHart, H. S. Gutowsky and T. C. Farrar, J. Am. Chem. Soc. 89, 5056 (1967).

10. W. E. Blumberg, Phys. Rev. 119, 79 (1960).

11. E. Fukushima and E. A. Uehling, Phys. Rev. 173, 366 (1968).

12. C. P. Slichter and D. Ailion, Phys. Rev. 135, A1099 (1964).

13. D. C. Look and I. J. Lowe, J. Chem. Phys. 44, 2995 (1966).

14. A. V. Chadwick and J. N. Sherwood, "Point Defects in Molecular Solids" in "Point Defects" (J. Crawford and L. Slifkin eds.), Consultants Bureau, 1973.

15. A. D. Britt, private communication.

16. R. K. Boyd, C. A. Fyfe, and D. A. Wright, J. Phys. Chem. Solids 35, 1355 (1974).

17. The constant term on the right hand side of Eq. [10] represents an average over some 30 solid substances in Table Ia of H. Hoyer and W. Peperle, Z. Elektrochem. 62, 61 (1958).

18. See Table 14 in A. Bondi, "Physical Properties of Molecular Crystals, Liquids and Glasses" Wiley & Sons, New York, 1968.

19. A. Stolovy, E. C. Jones, Jr., J. B. Aviles, Jr. and A. I. Namenson, NRL Report 8350 (1979).

20. B. M. Dobratz, "Properties of Chemical Explosives and Explosive Simulants" UCRL-51319 (1974); data from R. N. Rodgers (1974 private communication to B. M. Doloratz).

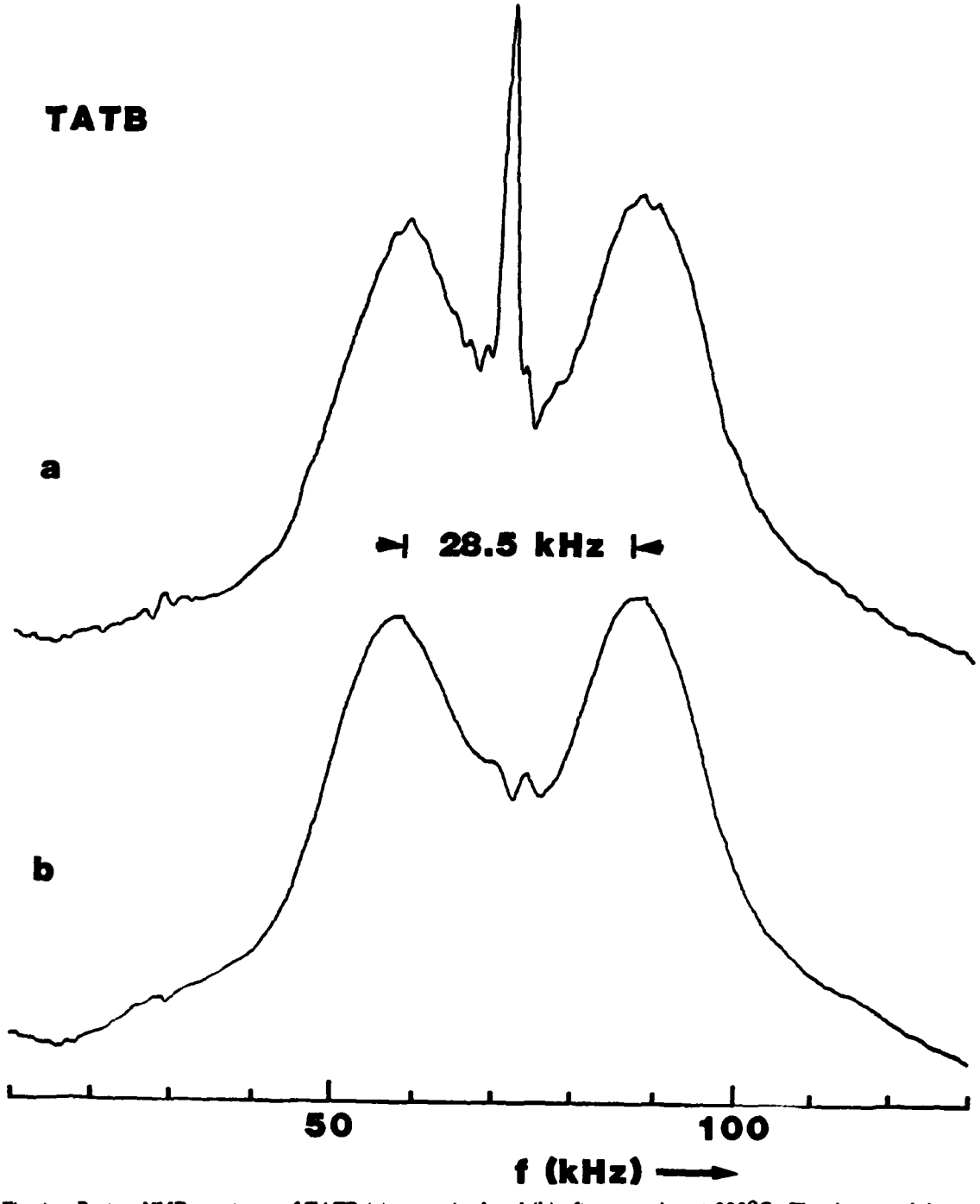

Fig. 1 — Proton NMR spectrum of TATB (a) as received and (b) after pumping at 200°C. The sharp peak in (a) is ascribed to water present in the processed material. A rather narrow proton resonance from the spectrometer probe has been subtracted off both (a) and (b), but the cancellation is not perfect and the features in the valley at about 75 kHz offset arise from this probe resonance and not TATB. The Pake doublet is characteristic of strongly coupled isolated spin pairs, here of the amino protons. The splitting of 28.5 kHz is derived from experimentally determined time of the first zero crossing of free induction decay (fid) and represents the separation of the *sharp peaks* in the Pake doublet.

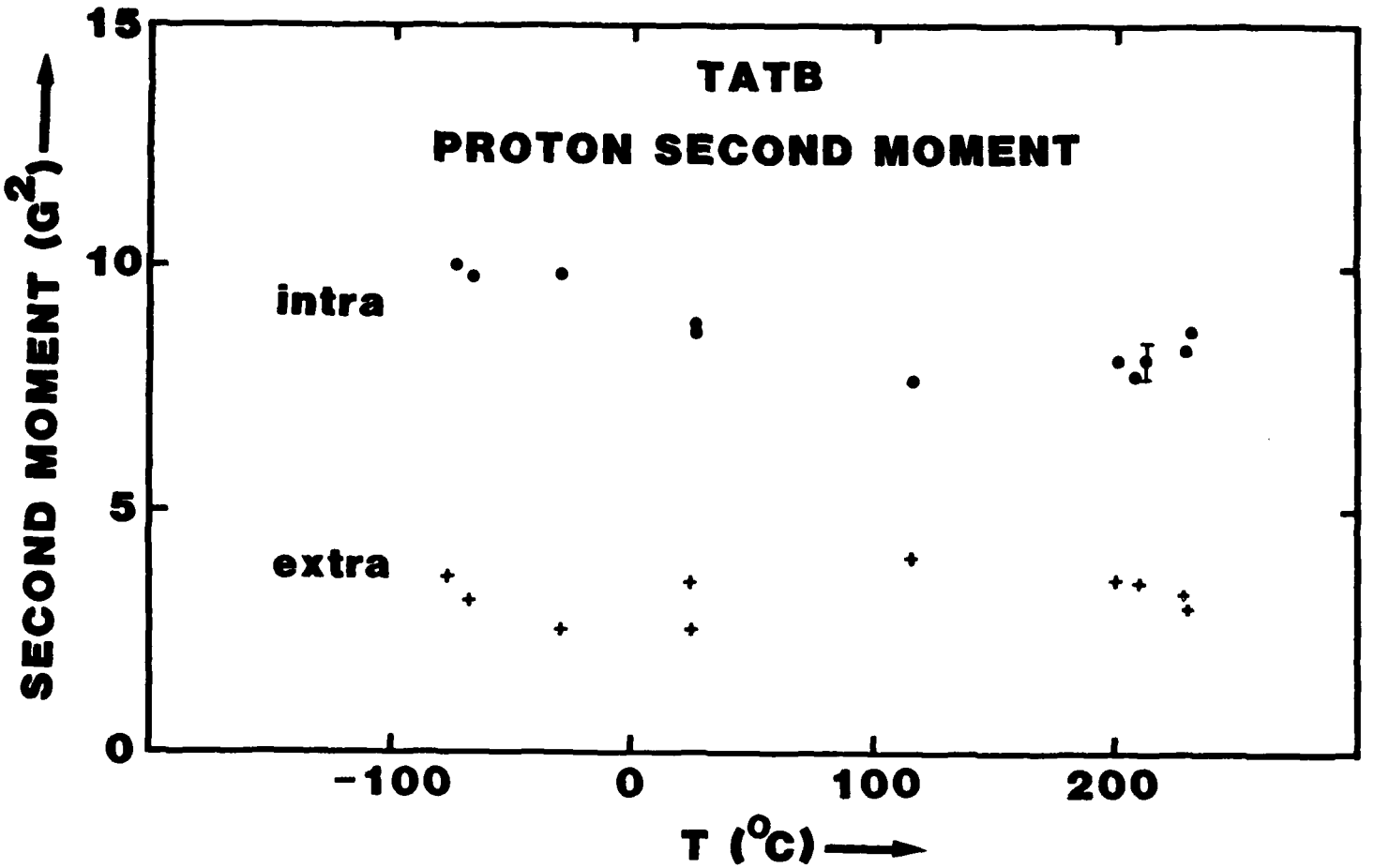

Fig. 2 — The proton second moment arising strictly from the amino proton pair (intra-pair) has been determined from the zero crossing of the fid. Gaussian broadening of the Pake doublet has been assumed and that broadening represents all other contributions (extra-pair) to the proton second moment. Both second moments are essentially temperature independent.

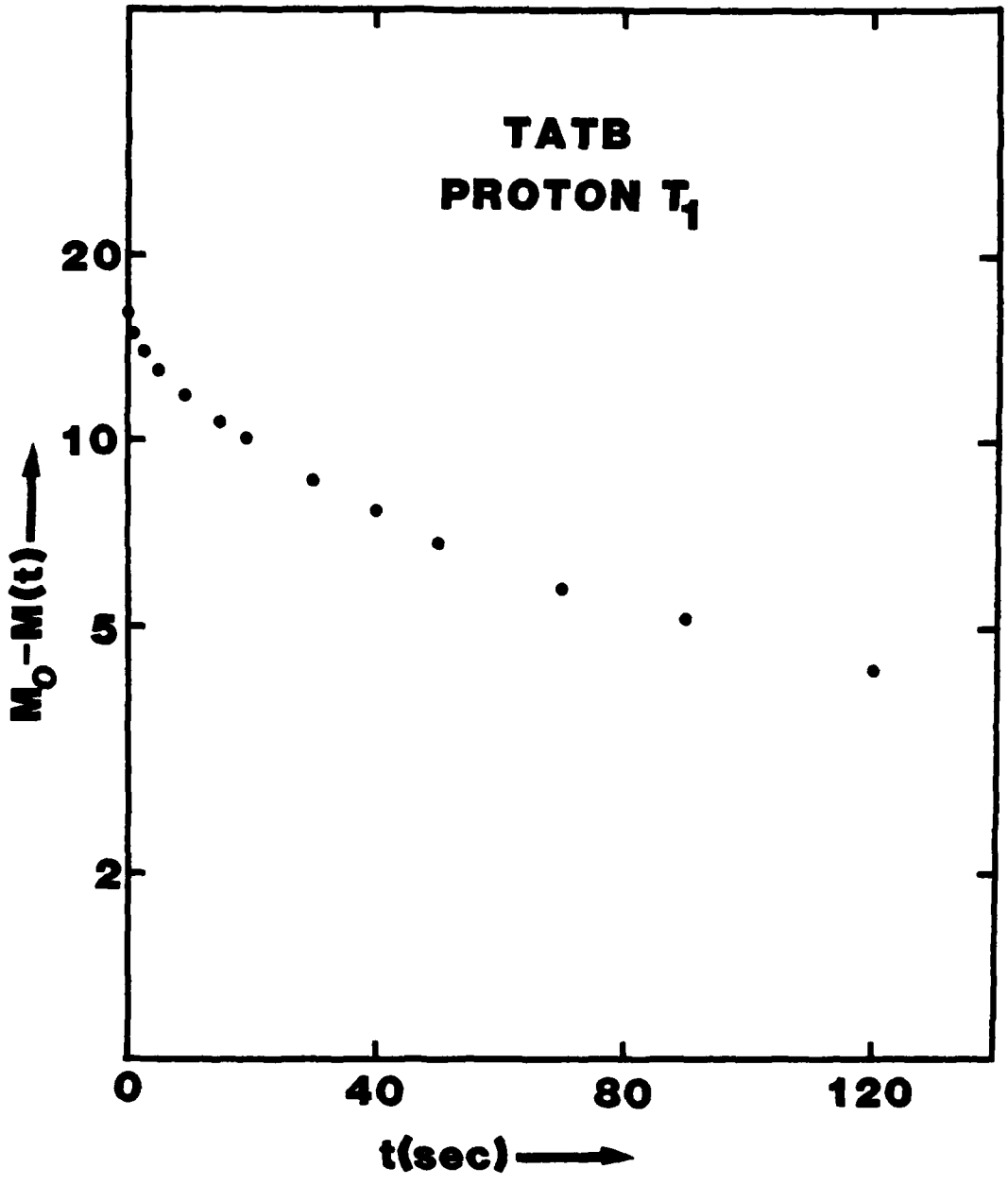

Fig. 3 — Magnetization versus time data for Zeeman spin-lattice relaxation (T_1) at 113°C. The recovery of magnetization is nonexponential; see also Figure 4. The total magnetization is represented by using the initial height of the fid.

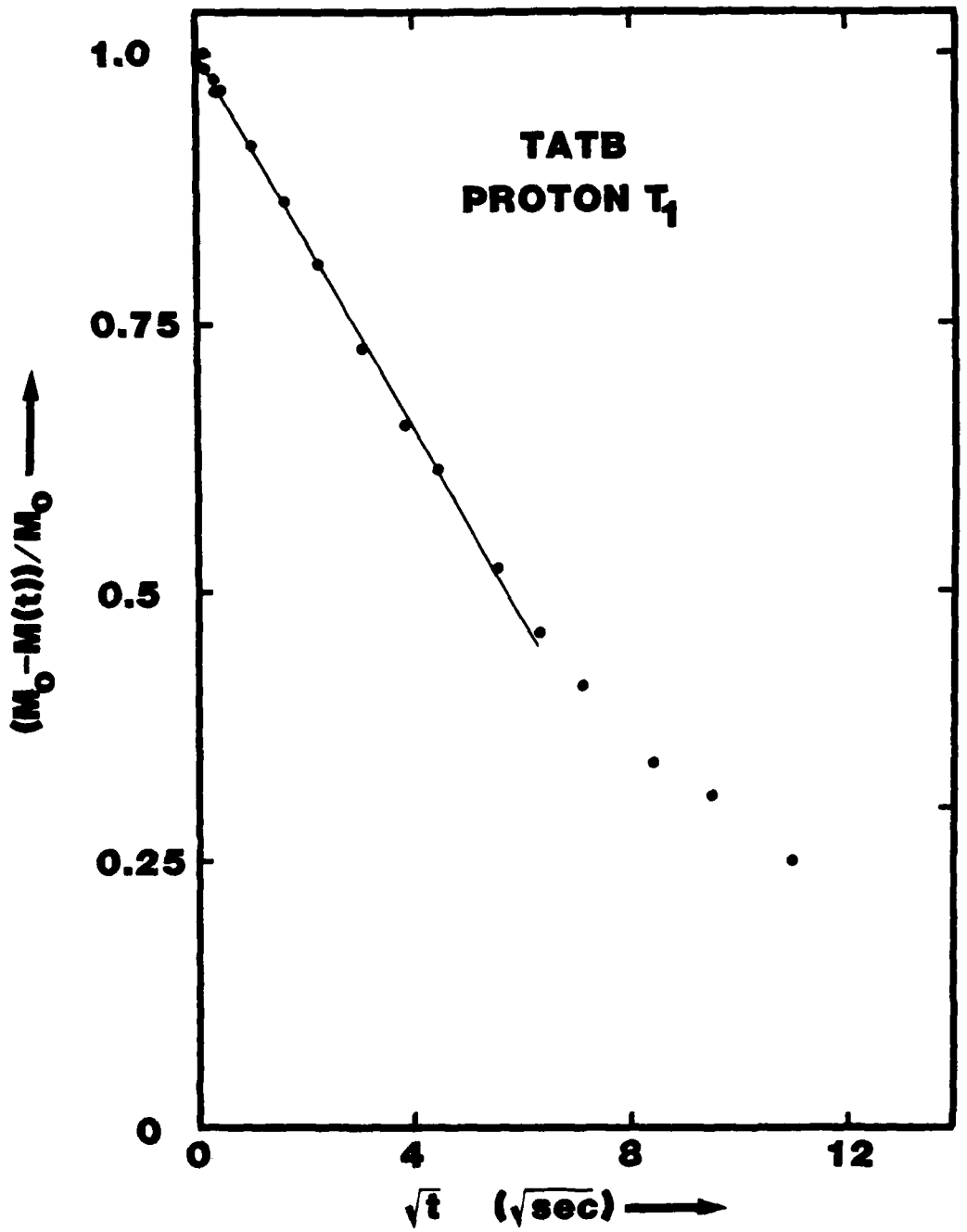

Fig. 4 — The T_1 magnetization data of Figure 3 are better fit by an M versus $(t/T_1)^{1/2}$ relation. The solid line corresponds to T_1 = 35 s.

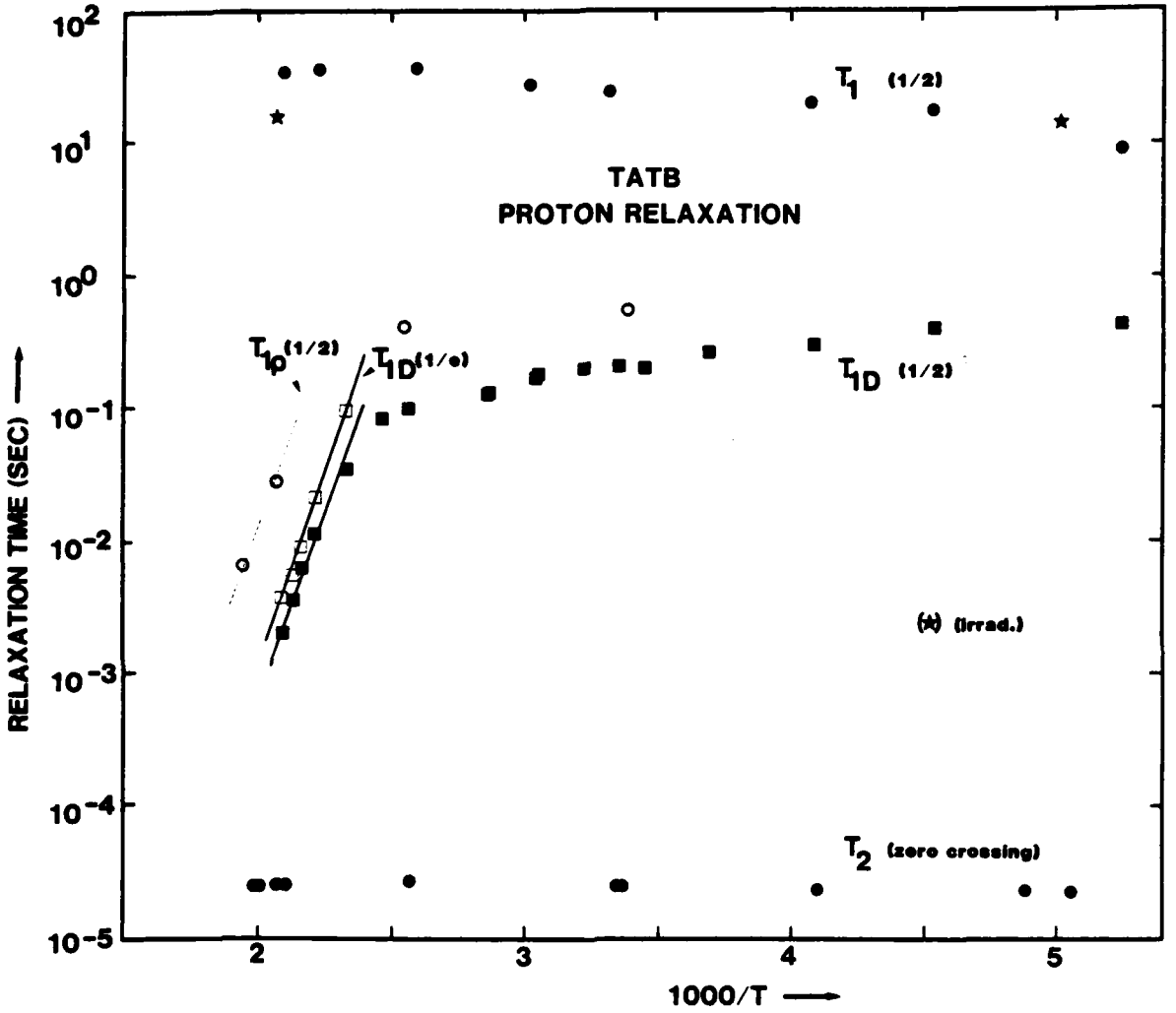

Fig. 5 — This figure summarizes the four relaxation times measured: T_2 (by zero crossing), dipolar spin-lattice time T_{1D}, rotating frame spin lattice time $T_{1\rho}$ and Zeeman spin-lattice time T_1. The nonexponential decays for T_{1D}, $T_{1\rho}$ and T_1 are characterized by the decay time to the one half point, except at high temperature for T_{1D} where the (1/e) values are also shown. The only evidence of molecular motion comes from the sharp drop in T_{1D} and $T_{1\rho}$ above about 150°C; the activation enthalpy is 120 kJ/mol. A γ-irradiated specimen shows a T_1 reduced by a factor of two, so indicating paramagnetic relaxation as the T_1 mechanism.

TABLE I

TATB Proton Second Moment Contributions at 26°C
(in G^2)

Proton Number[a]	Intra-Pair (theoretical[b])	Intra-Pair (experimental)	Extra-Pair ^1H-^1H (theoretical[b])	Extra-Pair ^{14}N-^1H (theoretical[b])	Extra-Pair ^{14}N-^1H (Experimental)
1	25.5 ± 10[c]		1.40	5.47 ± 2.7[c]	
2			1.53	4.46 ± 2.1	
3	23.3 ± 10		1.28	8.45 ± 4.4	
4			1.53	1.65 ± 0.85	
5	13.5 ± 6		1.34	4.46 ± 2.4	
6			1.89	1.56 ± 0.8	
Average over all protons	20.8 ± 5[c]	8.9 ± 0.4	1.50	4.3 ± 1[c]	3.1 ± 0.5

[a] Proton numbers follow the convention of Cady and Larson, Ref. 8. The average over the six protons is the contribution to total proton second moment.

[b] Theoretical values inferred from the x-ray determined distances of Ref. 8.

[c] We do not know how the uncertainties in the x-ray distances are correlated within the unit cell: here they are assumed uncorrelated.

TABLE II

T_1 Relaxation Across the TATB Proton Spectrum

Temperature	113°C	211°C (γ-irradiated)
	T_1[a](s)	T_1[a](s)
fid[b]	36	16
on resonance	32.5	15
peak	36	15
shoulder	41.5	18

[a] T_1 is shown here as the time to recover to one half of the value of the magnetization at thermal equilibrium, corresponding to a pulse delay time of 1000s.

[b] The initial part of the free induction decay (fid) measures the integrated spectrum.

TABLE III

Enthalpies of Activation and Sublimation[a]
(in kJ/mol)

Process	Rotation		Sublimation		Diffusion
Substance	ΔH_{rot} (expt)	ΔH_{rot} (calc)	ΔH_{sub} (expt)	ΔH_{sub} (calc)	$\Delta H_{diff.}$
Benzene	16	8.8-13	44.8	38-44	96[b]
Naphthalene	105	65-88	67.4-82.0	63-71	179[c]
Coronene	25	8-12	144	138-151	-
TATB	-	-	145[d]	180[e]	-

[a]Data taken from Ref. 16 unless indicated by other superscript.

[b]R. Fox and J. N. Sherwood, Trans. Farad Soc. 67, 3364 (1971) and F. Noack, M. Weithase and J. von Schütz, Z. Naturf. 30a, 1707 (1975).

[c]J. N. Sherwood and D. J. White, Phil. Mag. 16, 975 (1967).

[d]Deduced from vapor pressure estimate; see text.

[e]Calculated from functional group increments as described in text.